Semiconductor Physics, Quantum Electronics & Optoelectronics. 2002. V. 5, N 1. P. 51-57.

PACS: 73.20.-r, 73.30.+y,73.40.Lq

Production and investigation of Cu/thin intermediate tunnel-transparent dielectric oxide layer/n-$Pb_{0.935}Sn_{0.065}Te_{0.243}Se_{0.757}$/In Schottky barrier structures

A.I. Tkachuk, O.N. Tsarenko, S.I. Ryabets
Vynnychenko's Kirovograd State Pedagogical University, 1 Shevchenko St., 25006 Kirovograd, Ukraine
Phone: +380 (522) 24 8901; fax: +380 (522) 24 8544; e-mail: atkachuk@kspu.kr.ua

Abstract. The high-planar epitaxial layers of n-$Pb_{0.935}Sn_{0.065}Te_{0.243}Se_{0.757}$ quaternary solid solutions, lattice matched with {111}BaF_2 substrates, have been grown from bounded volume of supersaturated melt-solutions in the growth temperature region 773÷873 K by the liquid phase epitaxy technique at a programmatic refrigeration rate of 0.1÷0.2 K/min and a temperature reduction range of ΔT=5÷10 K. The laboratory methodology of the production of Cu/δ-layer/n-$Pb_{0.935}Sn_{0.065}Te_{0.243}Se_{0.757}$/In Schottky barrier structures by thermal vacuum deposition has been developed. The current- and farad-voltage characteristics of these structures have been measured at the 77 K, and the dependence of the diode electro-physical properties on the δ-layer width has been studied.

Keywords: lead-tin chalcogenide; liquid phase epitaxy; Schottky barrier structures; intermediate oxide layer.

Paper received 29.10.01; revised manuscript received 21.12.01; accepted for publication 05.03.02.

1. Introduction

The metal/lead-tin chalcogenide contacts with Schottky barrier provide a convenient and relatively inexpensive method to fabricate high-quality infrared photodiodes for application in the wavelength region 8÷14 μm of the atmospheric window [1-3]. At the same time, these barrier structures have been only partially studied for the In (Pb, In-Ag)/p-$Pb_{1-x}Sn_xTe$/Au [2-5], Pb/p-$Pb_{1-x}Sn_xSe$/Pt(Au) [6-9] and Pb/p-$PbTe_{1-y}Se_y$/Pt [7, 10] junctions on the basis of epitaxial layers, which were grown on {111}BaF_2 and {111}Si (with CaF_2-SrF_2-BaF_2 buffer layer) substrates by the molecular beam or hot wall epitaxy. But the information about the production and the properties of the Schottky diodes on the basis of epitaxial layers of the $Pb_{1-x}Sn_xTe_{1-y}Se_y$ quaternary solid solutions, which were grown on BaF_2 by the liquid phase epitaxy technique, is absent. Furthermore, most of the authors, when interpreting obtained electro-physical and optical experimental characteristics of these barrier structures, use only ideal Schottky barrier model and disregard by the available thin intermediate tunnel-transparent dielectric oxide layer (δ-layer). This layer is usually formed on the lead-tin chalcogenide surface during chemical polishing or exposing to the ambient atmosphere prior to the vacuum deposition of the barrier metal. However, practically, metal/lead-tin chalcogenide Schottky barrier diodes with δ-layer have better characteristics [11-13], moreover, the values of zero bias resistance area product (R_0A) and zero bias built-in potential (φ^o_{bi}) increase with increase of δ-layer width [11,13]. The absence of δ-layer may be reduced to the degradation of the metal/lead-tin chalcogenide interface and deterioration of rectificational properties of the Schottky diode as the result of chemical interaction between deposited barrier metal and semiconductor material [5, 11, 12].

In accordance with [14], surfaces of the $Pb_{1-x}Sn_xTe$ and $Pb_{1-x}Sn_xSe$ solid solutions oxidize at the atmospheric pressure and room temperature rather quickly with formation PbO, SnO_2, TeO_2, SeO_2 oxides and acceptor surface states. The composition and thickness of δ-layer depend on the air exposition time, and it is known that tin

© 2002, Institute of Semiconductor Physics, National Academy of Sciences of Ukraine

oxidize in the quickest way but lead – in the slowest [13, 14]. It should be taken into account at the analysis of experimental data, while the surface state density decreases with increasing the δ-layer width and changing its composition [11].

The main goal of this work was to search and develop the laboratory methodology of the production of Cu/δ-layer/n-$Pb_{0.935}Sn_{0.065}Te_{0.243}Se_{0.757}$/In Schottky barrier structures based high-quality epitaxial layers of n-$Pb_{0.935}Sn_{0.065}Te_{0.243}Se_{0.757}$ quaternary solid solutions. using industrial and original equipment for liquid phase epitaxy and thermal vacuum deposition. Besides, we had to study the dependence of electro-physical characteristics of respective diodes on the δ-layer width.

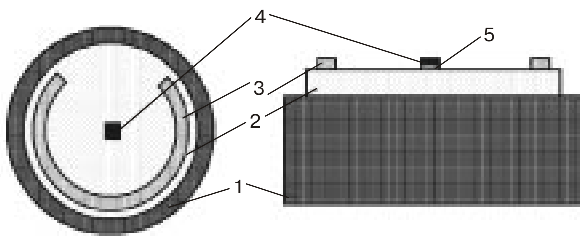

Fig. 1 Schematic view of the Cu/δ-layer/n-$Pb_{0.935}Sn_{0.065}Te_{0.243}Se_{0.757}$/In Schottky barrier structures:1 - {111}BaF_2 substrate; 2 - epitaxial layers of n-$Pb_{0.935}Sn_{0.065}Te_{0.243}Se_{0.757}$; 3 - ohmic In contact; 4 - rectifying Cu contact; 5 - δ-layer.

2. Experimental procedure

The epitaxial layers of n-$Pb_{0.935}Sn_{0.065}Te_{0.243}Se_{0.757}$ quaternary solid solutions, lattice matched with {111}BaF_2 substrates, were grown from bounded volume of $(Pb_{1-v}Sn_v)_{1-w}(Te_{1-u}Se_u)_w$ melt-solutions in the growth temperature region 773÷873 K by the liquid phase epitaxy (LPE) technique at the programmatic refrigeration of the growth solution. The LPE processes were performed in a vertical reactor, placed into a furnace with a resistive heater, in the flow of hydrogen purified by a palladium filter. A special blacklead crucible and cylindrical rotating cassette were used for the LPE growth of high-planar n-$Pb_{0.935}Sn_{0.065}Te_{0.243}Se_{0.757}$ epitaxial layers. The BaF_2 dielectric substrates were obtained by the spalling of Bridgman monocrystals in the direction of the {111} crystallographic plane and dynamic-chemical polishing of their surfaces in the 10% aqueous solution of HNO_3. These substrates had the form of washer with 20 mm in diameter and 2÷5 mm in thickness. Their surface dislocation densities were $N_d=(4÷8)\times10^4$ cm^{-2}. {111}BaF_2 substrates were laid on the vertical rotating blacklead cassette in pairs with 1÷2 mm clearance. The $(Pb_{1-v}Sn_v)_{1-w}(Te_{1-u}Se_u)_w$ melt-solutions were prepared from elemental lead, tin, tellurium and selenium of highest purity grade. Sn, Se and chalcogenide contents in the liquid phase were varied within the ranges $0.073\le v\le0.078$, $0.403\le u\le0.420$ and $0.01\le w\le0.04$ atomic fractions, respectively. After the melt-solution was homogenized in blacklead crucible during 2 hours at the temperature 2÷3 K higher than the liquidus ones, the epitaxy growth was initiated 1÷2 K below the liquidus temperature by filling of the melt-solution on the substrates through the slot of cassette. The range of the temperature reduction was ΔT=5÷10 K at a programmatic refrigeration rate of 0.1÷0.2 K per minute. The melt-solution was removed from the growth surface by centrifugation.

The obtained $Pb_{0.935}Sn_{0.065}Te_{0.243}Se_{0.757}$ epitaxial layers had the thickness of h=3÷7 mm, surface dislocation density $N_d<10^5$ cm^{-2}, n-type conduction, band gap energy $E_g=0.124$ eV, electron concentration $n=(2.2÷2.7)\times10^{17}$ cm^{-3} and Hall mobility $\mu=(8.3÷9.1)\times10^3$ $cm^2V^{-1}s^{-1}$ at 77 K.

Ohmic and rectifying contacts to the n-$Pb_{0.935}Sn_{0.065}Te_{0.243}Se_{0.757}$ epitaxial layers were obtained by the thermal deposition of indium and copper in the vacuum of about $10^{-5}÷10^{-6}$ Torr through the system of stainless-steel masks at a rate of about 500 Å per minute and 1800 Å per minute, respectively. The In contacts had a large area of about 50.2 mm^2 and the thickness of about 3000 Å. Prior to the deposition of In contacts, the epitaxial layers were vacuum annealed at 423 K for about 1800 seconds to desorb a surface oxide layer. After the deposition of In contacts and before to the deposition of Cu contacts, the thin intermediate tunnel-transparent dielectric oxide layers on the epitaxial layer surfaces were formed by the forced oxidation at 473 K during 10÷1200 sec. The obtained Cu rectifying contacts had the thickness of about 2000÷3000 Å and an active area A of about 2.25 mm^2. In Fig. 1 a schematic view of Cu/δ-layer/n-$Pb_{0.935}Sn_{0.065}Te_{0.243}Se_{0.757}$/In Schottky barrier structures are shown. For electrical measurements, the thin copper wires with diameter of about 0.1 mm were mounted to the ohmic and rectifying contacts with the help of solder 52%In + 47% Sn + 1% Ag. The current-voltage characteristics (CVC) of the Cu/δ-layer/n-$Pb_{0.935}Sn_{0.065}Te_{0.243}Se_{0.757}$/In Schottky barrier structures were measured at the direct current and 77 K. The farad-voltage characteristics (FVC) were measured by the bridge method at the frequency f=1MHz and 77 K.

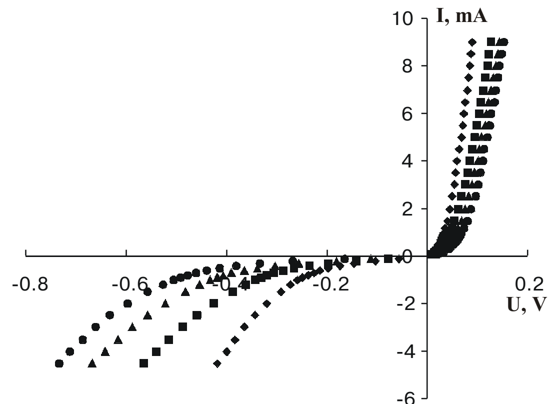

Fig. 2 CVC of the Cu/δ-layer/n-$Pb_{0.935}Sn_{0.065}Te_{0.243}Se_{0.757}$ /In Schottky barrier structures at 77 K (♦ - structure №1; ▲ - structure №2; ■ - structure №3; • - structure №4).

Table1. Parameters of the Cu/δ-layer/n-$Pb_{0.935}Sn_{0.065}Te_{0.243}Se_{0.757}$/In Schottky barrier structures at 77 K.

№	t, sec	R_0A, Ωcm^2	r, Ω	I_S, $\times 10^{-5}$A	β	C_0, $\times 10^{-9}$F	U_I, V	φ^o_{bi}, V	δ, Å
1	180	2.9	3.9	9.2	1.8	6.69	0.092	0.058	199
2	370	4.7	6.3	7.1	2.2	4.53	0.137	0.069	268
3	690	7.5	5.7	5.5	2.7	3.41	0.203	0.082	431
4	1020	10.1	4.2	4.4	3.1	2.89	0.262	0.091	592

3. Results and discussions

For the forward voltage bias 0.02<U<0.16 V, the experimental current-voltage curves of the Cu/δ-layer/n-$Pb_{0.935}Sn_{0.065}Te_{0.243}Se_{0.757}$/In Schottky barrier structures were good approximated by the expression:

$$I = I_S \exp\left[\frac{q(U - Ir)}{\beta kT}\right] \quad [A], \qquad (1)$$

where ideality coefficient β and saturation curcurrent I_S ranged for the various structures within the limits from 1.8 to 3.1 and from 91 to 35 μA. The maximum value of the zero bias resistance area product was about 10.6 Ωcm^2. Series resistance r, that is determined by the resistance of the semiconductor quasi-neutral region, ohmic contact resistance and spreading resistance, taken on a value 3.9÷6.3 Ω. In Fig. 2 shown are the typical CVC with the example of four selected barrier structures with the different oxidation time t. Measured values of the R_0A, r, I_S and β of these diodes were reduced in the Table with the same numeration of structures as in Fig 2. The reverse branches of the CVC did not saturate and had the view, which is typical for the "soft breakdown" [12, 15].

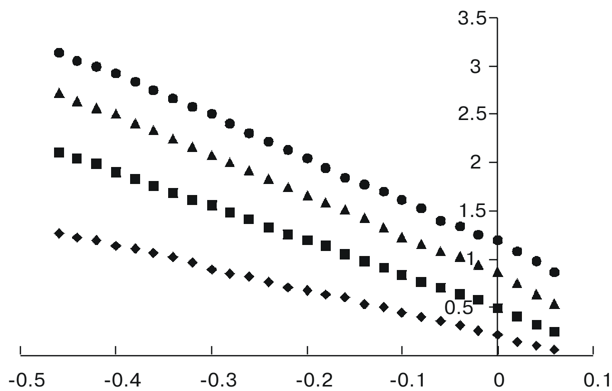

Fig. 3 FVC of the Cu/δ-layer/n-$Pb_{0.935}Sn_{0.065}Te_{0.243}Se_{0.757}$ /In Schottky barrier structures at 77 K (♦ - structure №1; ▲- structure №2; ■ - structure №3; • - structure №4).

For the reverse voltage biases $-0.4<U<0$ V, the experimental FVC plots of Cu/δ-layer/n-$Pb_{0.935}Sn_{0.065}Te_{0.243}Se_{0.757}$/In Schottky barrier structures were good approximated by the expression:

$$C^{-2} = B\beta\left[\beta\left(\varphi^0_{bi} - \frac{kT}{q}\right) - U\right] \quad [F^{-2}], \qquad (2)$$

where coefficient B ranged within the limits from 1.31×10^{17} to 1.62×10^{17} $C^{-2}V^{-1}$, which may be explained by different values of the product of ionized donor concentration into semiconductor dielectric permittivity for various structures. In Fig. 3, the typical FVC on the example of the same four selected barrier structures are shown. For the determination of zero bias built-in potentials from the relationship [12]:

$$\varphi^0_{bi} = \frac{U_I}{\beta} + \frac{kT}{q} \quad [V], \qquad (3)$$

the intercept voltages U_I were obtained by extrapolation of the line section of FVC plots onto the abscissa. Measured values of the B, U_I, φ^o_{bi} and zero bias capacitance (C_0) for the four selected Cu/δ-layer/n-$Pb_{0.935}Sn_{0.065}Te_{0.243}Se_{0.757}$/In Schottky barrier structures are given in Table, too.

As the explanation of the obtained experimental results, we proposed a physical model of the Cu/δ-layer/n-$Pb_{1-x}Sn_xTe_{1-y}Se_y$/In Schottky barrier structure. Constructing this model we proceeded on the assumptions that: δ-layer is the tunnel-transparent for the electrons and its influence reduce only to potential drop on it ($\Delta\varphi_i$); surface state continuous distribution on the δ-layer/n-$Pb_{1-x}Sn_xTe_{1-y}Se_y$ interface is characterized by the electrical neutrality level (φ_0) – filling level of the surface state band by electrons at the thermodynamic equilibrium between δ-layer and n-$Pb_{1-x}Sn_xTe_{1-y}Se_y$ before the deposition of copper and after the deposition of indium contacts; after the deposition of copper, the surface states on the δ-layer/n-$Pb_{1-x}Sn_xTe_{1-y}Se_y$ interface interact well with states in the metal conduction band at the expense of tunneling, because of that the surface state filling is determined by metal Fermi level (E_{FCu}) and the surface states become the acceptor surface states (the electrical neutrality level in the state of the thermodynamic equilibrium is already placed below the semiconductor Fermi level E_{FS}); the energetic density of surface states D_S [$J^{-1}m^{-2}$] is a constant in the energy interval from φ_0 to E_{FCu}; the electric field strength in the δ-layer is a constant in the state of the thermodynamic equilibrium ($E_i^0(x)$= const); general charge in the barrier layer consists of the sum of uniform completely ionized donor motionless charge, free-electron charge (majority carrier) and free hole charge (minority carrier). So, width, electric field

strength and electric field potential of the barrier layer of Cu/δ-layer/n-$Pb_{1-x}Sn_xTe_{1-y}Se_y$/In Schottky barrier structure are assigned by expressions [15,16,18]:

$$L(x)=\left[\frac{2\varepsilon_0\varepsilon_S}{qN_D}\left(\varphi_{bi}{}^0-\frac{kT}{q}-U_d\right)\right]^{\frac{1}{2}} \quad [\text{m}],$$

$$E_S(x)=-\frac{qN_D}{\varepsilon_0\varepsilon_S}(L-x) \quad [\text{Vm}^{-1}], \qquad (4)$$

$$\varphi_S(x)=\frac{qN_d}{2\varepsilon_0\varepsilon_S}(L-x)^2 \quad [\text{V}],$$

where q is the electronic charge; N_D - ionized donor concentration; ε_S - relative static dielectric permittivity of semiconductor; U_d – voltage drop on the barrier layer; x – distance, which is counted off from δ-layer/n-$Pb_{1-x}Sn_xTe_{1-y}Se_y$ interface into the semiconductor.

In Fig. 4 the qualitative energy-band diagrams of the Cu/δ-layer/n-$Pb_{1-x}Sn_xTe_{1-y}Se_y$/In Schottky barrier structure are shown for the zero (a), forward (b) and reverse (c) voltage biases, where: $E_{Cu}{}^0$, $E_S{}^{00}$ ($E_S{}^{0F}$, $E_S{}^{0R}$) and $E_{In}{}^0$ - zero level of the Cu, n-$Pb_{1-x}Sn_xTe_{1-y}Se_y$ and In, respectively; $E_{CS}{}^0$ ($E_{CS}{}^F$, $E_{CS}{}^R$) – conduction band edge of the semiconductor; E_{FCu} and E_{FIn} – Fermi level of the Cu and In; $E_{FS}{}^0$ and $E_{FS}{}^F$($E_{FS}{}^R$) - Fermi level (at the zero bias) and quasi-Fermi level (at the forward/reverse bias) of the semiconductor lying μ_S [J] below the conduction band edge; $E_{VS}{}^0$ ($E_{VS}{}^F$, $E_{VS}{}^R$) – valance band edge of the n-$Pb_{1-x}Sn_xTe_{1-y}Se_y$; A_{Cu}, A_S and A_{In} – work function of the Cu, semiconductor and In, respectively; χ_S – electron affinity of the n-$Pb_{1-x}Sn_xTe_{1-y}Se_y$; E_g – band gap energy of the semiconductor; $U_d{}^F$ ($U_d{}^R$) – voltage drop on the barrier layer; $U_i{}^F$ ($U_i{}^R$) - voltage drop on the δ-layer; φ_0 - electrical neutrality level; $q\Delta\varphi_i{}^0$ ($q\Delta\varphi_i{}^F$, $q\Delta\varphi_i{}^R$) – potential drop on the δ-layer; $q\varphi_{bi}{}^0$ ($q\varphi_{bi}{}^F$, $q\varphi_{bi}{}^R$) - built-in potential; $q\varphi_b{}^0$ ($q\varphi_b{}^F$, $q\varphi_b{}^R$) – barrier height; $q\Delta\varphi_{bi}{}^0$ ($q\Delta\varphi_{bi}{}^F$, $q\Delta\varphi_{bi}{}^R$) - built-in potential lowering due to image forces; ε_i - relative static dielectric permittivity of the δ-layer; δ – δ-layer width; L^0 (L^F, L^R) - barrier layer width; $Q_{SC}{}^0$ ($Q_{SC}{}^F$, $Q_{SC}{}^R$) - surface density of the barrier layer charge; $Q_{SS}{}^0$ ($Q_{SS}{}^F$, $Q_{SS}{}^R$) - charge density of the acceptor surface states; $Q_{Cu}{}^0$ ($Q_{Cu}{}^F$, $Q_{Cu}{}^R$) - charge surface density on the active surface of the Cu barrier contact.

The electrical neutrality condition of the Cu/δ-layer/n-$Pb_{1-x}Sn_xTe_{1-y}Se_y$ Schottky barrier contact at the zero bias (Fig. 4, a) can be written [15, 16]:

$$Q_{Cu}^0+Q_{SS}^0+Q_{SC}^0=0 \ [\text{Cm}^{-2}], \qquad (5)$$

where

$$Q_{Cu}^0=-\frac{\varepsilon_0\varepsilon_i}{q\delta}\left(A_{Cu}-A_S-q\varphi_{bi}^0\right) \ [\text{C m}^{-2}];$$

$$Q_{SS}^0=-qD_S\left(E_g-\varphi_0-\mu_S-q\varphi_{bi}^0\right)[\text{C m}^{-2}]; \qquad (6)$$

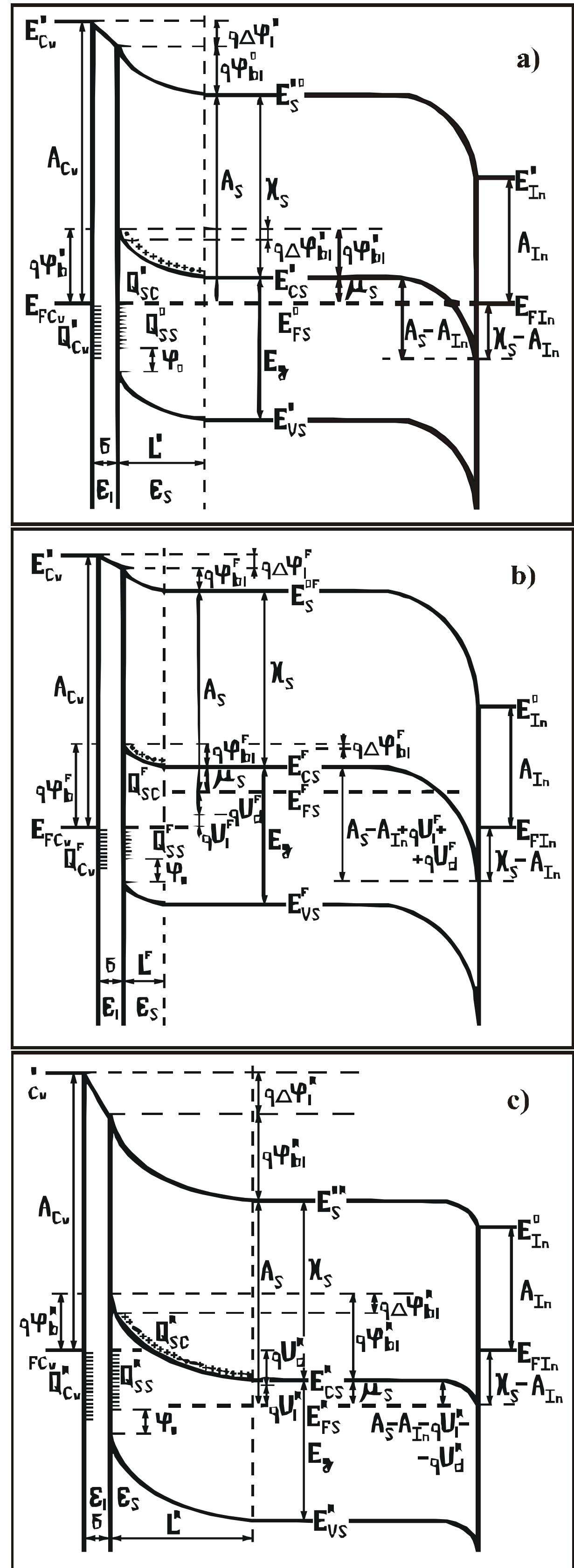

Fig. 4 Qualitative energy-band diagrams of the Cu/δ-layer/n-$Pb_{1-x}Sn_xTe_{1-y}Se_y$/In Schottky barrier structure for the zero (a), forward (b) and reverse (c) voltage bias.

$$Q_{SC}^{0}=\left[2\varepsilon_0\varepsilon_S qN_D\left(\varphi_{bi}^{0}-\frac{kT}{q}\right)\right]^{\frac{1}{2}} \quad [\mathrm{C\,m^{-2}}].$$

From (5) and (6) we have:

$$\varphi_{bi}^{0}=\varphi_1+\alpha-\left[\alpha^2+2\alpha\left(\varphi_1-\frac{kT}{q}\right)\right]^{\frac{1}{2}} \quad [\mathrm{V}],$$

$$\varphi_{b}^{0}=\varphi_1+\alpha+\frac{\mu_S}{q}-\left[\alpha^2+2\alpha\left(\varphi_1-\frac{kT}{q}\right)\right]^{\frac{1}{2}} \quad [\mathrm{V}], \quad (7)$$

$$\Delta\varphi_{i}^{0}=\frac{1-\gamma}{q}\left(A_{Cu}-A_S-E_g+\varphi_0+\mu_S\right)-\alpha+ +\left[\alpha^2+2\alpha\left(\varphi_1-\frac{kT}{q}\right)\right]^{\frac{1}{2}} \quad [\mathrm{V}],$$

where

$$\varphi_1=\frac{1}{q}\left[\gamma\left(A_{Cu}-A_S\right)+\left(1-\gamma\right)\left(E_g-\varphi_0-\mu_S\right)\right] \quad [\mathrm{V}],$$

$$\gamma=\frac{\varepsilon_0\varepsilon_i}{\varepsilon_0\varepsilon_i+q^2\delta D_S}; \quad \alpha=\frac{qN_D\varepsilon_0\varepsilon_S\delta^2}{\left(\varepsilon_0\varepsilon_i+q^2\delta D_S\right)^2} \quad [\mathrm{V}]. \quad (8)$$

In the case when the forward (reverse) voltage bias U has been applied to the Cu/δ-layer/n-$Pb_{1-x}Sn_xTe_{1-y}Se_y$/In Schottky barrier structure (Fig. 4,b,c), the electrical neutrality condition (2) can be rewritten:

$$Q_{Cu}+Q_{SS}+Q_{SC}=0 \quad [\mathrm{C\,m^{-2}}], \quad (9)$$

where

$$Q_{Cu}=-\frac{\varepsilon_0\varepsilon_i}{q\delta}\left(A_{Cu}-A_S-q\varphi_{bi}-qV\right) \quad [\mathrm{C\,m^{-2}}];$$

$$Q_{SS}=-qD_S\left(E_g-\varphi_0-\mu_S-q\varphi_{bi}-qV\right)[\mathrm{C\,m^{-2}}];$$

$$Q_{SC}=\left[2\varepsilon_0\varepsilon_S qN_D\left(\varphi_{bi}-\frac{kT}{q}\right)\right]^{\frac{1}{2}} [\mathrm{C\,m^{-2}}]; \quad (10)$$

$$\varphi_{bi}=\varphi_{bi}^{0}-U_d \ [\mathrm{V}]; \quad \Delta\varphi_i=\Delta\varphi_i^{0}-U_i \ [\mathrm{V}];$$

$$\varphi_b=\varphi_b^{0}+U_i \ [\mathrm{V}]; \quad U=U_i+U_d+U_b [\mathrm{V}];$$

$V=U_d+U_i=U-U_b$ [V]; U_b - voltage drop on the series resistance r (Fig. 5).

From (9) and (10) we have:

$$\varphi_{bi}=\varphi_1+\alpha-V-\left[\alpha^2+2\alpha\left(\varphi_1-\frac{kT}{q}-V\right)\right]^{\frac{1}{2}} \quad [\mathrm{V}];$$

$$\varphi_{b}=\varphi_1+\alpha+\frac{\mu_S}{q}-\left[\alpha^2+2\alpha\left(\varphi_1-\frac{kT}{q}-V\right)\right]^{\frac{1}{2}} \quad [\mathrm{V}];$$

$$U_d=V+\left[\alpha^2+2\alpha\left(\varphi_1-\frac{kT}{q}-V\right)\right]^{\frac{1}{2}}- -\left[\alpha^2+2\alpha\left(\varphi_1-\frac{kT}{q}\right)\right]^{\frac{1}{2}} \quad [\mathrm{V}], \quad (11)$$

$$U_i=\left[\alpha^2+2\alpha\left(\varphi_1-\frac{kT}{q}\right)\right]^{\frac{1}{2}}- -\left[\alpha^2+2\alpha\left(\varphi_1-\frac{kT}{q}-V\right)\right]^{\frac{1}{2}} \quad [\mathrm{V}];$$

$$\Delta\varphi_{i}=\frac{1-\gamma}{q}\left(A_{Cu}-A_S-E_g+\varphi_0+\mu_S\right)-\alpha+ +\left[\alpha^2+2\alpha\left(\varphi_1-\frac{kT}{q}-V\right)\right]^{\frac{1}{2}} \quad [\mathrm{V}].$$

So, from the Fig. 4 and expressions (11) it follows that the barrier height of the Cu/δ-layer/n-$Pb_{1-x}Sn_xTe_{1-y}Se_y$/In Schottky barrier structure ($q\varphi_b$) depends on the applied voltage bias and decreases with increase of the reverse bias. It explains the absence of reverse branch saturation of the experimental CVC (Fig. 2). Furthermore, the built-in potential lowering due to image forces ($\Delta\varphi_{bi}$) can also influence on the appearance of current-voltage curves.

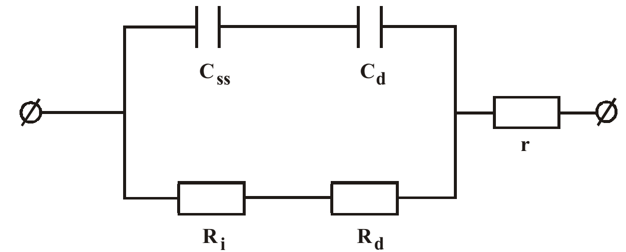

Fig. 5. Equivalent circuit of the Cu/δ-layer/n-$Pb_{1-x}Sn_xTe_{1-y}Se_y$/In Schottky barrier structure: R_i - δ-layer resistance; R_d - differential resistance of the barrier layer; C_{SS} - surface state capacitance; C_d - differential capacitance of the barrier layer; r - series resistance.

In accordance with [15-20], the barrier reduction can be calculated from the relationship for the summation potential energy on the interface of δ-layer/n-$Pb_{1-x}Sn_xTe_{1-y}Se_y$:

$$q\varphi_\Sigma(x)=q\varphi_S(x)+q\varphi^*(x) \quad [\mathrm{J}], \quad (12)$$

where $q\varphi^*(x)=\dfrac{q^2(\varepsilon_i-\varepsilon_S)}{16\pi\varepsilon_0\varepsilon_S(\varepsilon_i+\varepsilon_S)x}$ [J] – potential energy of the image forces. Proceeding on the assumption that $q\varphi\Sigma(x)$ extremum places in the x_{max}<<L, then the built-in potential lowering due to image forces can be written:

$$\Delta\varphi_{bi} = \left[\left(\frac{\varepsilon_S - \varepsilon_i}{\varepsilon_S + \varepsilon_i}\right)^2 \frac{q^3 N_D}{8\pi^2 \varepsilon_0^3 \varepsilon_S^3}\left(\varphi_{bi} - \frac{kT}{q}\right)\right]^{\frac{1}{4}} \text{ [V]}, \quad (13)$$

Thus, $\Delta\varphi_{bi}$ depends on the $\varphi_{bi}(V)$ and increase with the increasing reverse bias, as shown in Fig. 4.

In the general case, the current through the Cu/δ-layer/ n-$Pb_{1-x}Sn_xTe_{1-y}Se_y$/In Schottky barrier structure can be described by the expression [18-20]:

$$I = I_S\left[\exp\left(\frac{qV}{\beta kT}\right) - \exp\left(-\frac{qV}{\beta^{/} kT}\right)\right] \text{ [A]}, \quad (14)$$

and can be determined by: charge carrier emission over the barrier of depletion layer; charge carrier tunnelling through the barrier of depletion layer; charge carrier generation or recombination in the barrier layer; resonance tunnelling of charge carrier through the localized levels in the barrier layer; hole recombination and generation in the quasi-neutral region of semiconductor; passage of charge carrier through the surface states; charge carrier tunnelling through the barrier of δ-layer; passage of charge carrier over the barrier of δ-layer. If $d(\ln I_S)/dV \approx 0$, then ideality coefficients of CVC may be calculated as:

$$\frac{1}{\beta} = \frac{dU_d}{dV} = 1 - \alpha\left[\alpha^2 + 2\alpha\left(\varphi_1 - \frac{kT}{q} - V\right)\right]^{-\frac{1}{2}} \quad (15)$$

$$\frac{1}{\beta^{/}} = \frac{dU_i}{dV} = \alpha\left[\alpha^2 + 2\alpha\left(\varphi_1 - \frac{kT}{q} - V\right)\right]^{-\frac{1}{2}} = 1 - \frac{1}{\beta} \quad (16)$$

and expression (14) at the $V \geq 3kT/q$ can be rewritten:

$$I = I_S \exp\left(\frac{qV}{\beta kT}\right) \text{ [A]}, \quad (17)$$

that agrees well with the obtained experimental results.

Capacitance of the Cu/δ-layer/n-$Pb_{1-x}Sn_xTe_{1-y}Se_y$/In Schottky barrier structure consists of two capacitances (Fig. 5), which are connected in series [17-20]:

$$\frac{1}{C} = \frac{1}{C_{SS}} + \frac{1}{C_d} \quad (18)$$

where

$C_{SS} = \dfrac{A\left(\varepsilon_0 \varepsilon_i + q^2 \delta D_S\right)}{\delta}$ - surface state capacitance;

$C_d = \dfrac{A\varepsilon_0 \varepsilon_S}{L}$ - differential capacitance of the barrier layer.

Finally combining (11), (16) and (18) we have:

$$C = \frac{A\varepsilon_0 \varepsilon_i (\beta - 1)}{\delta\gamma\beta} \text{ [F]}. \quad (19)$$

This expression gives the possibility to obtain the relationship for the calculation of assessmentive value of δ-layer width:

$$\delta = \frac{\varepsilon_0 \varepsilon_i}{\dfrac{C\beta}{A(\beta - 1)} - q^2 D_S} \text{ [m]}. \quad (20)$$

Calculated assessmentive values of δ-layer width for the selected Cu/δ-layer/n-$Pb_{0.935}Sn_{0.065}Te_{0.243}Se_{0.757}$/In Schottky barrier structures are reduced in Table.

Form the Fig. 2, Fig. 3 and Table, it is apparent that the R_0A, β, U_I, φ^o_{bi} increase and I_S, C_0 decrease with the increasing δ-layer width. Furthermore, the current value I at one and the same voltage bias U decrease with the increasing δ-layer width. It may be explaned by corresponding increase of the δ-layer barrier and dependence of the barrier height $q\varphi_b$ on the values of relative static dielectric permittivity of the δ-layer, δ-layer width and density of surface states (see expressions (8) and (11)). Increasing of the zero bias built-in potential with the increasing δ-layer width may be explained by the decreasing density of surface states and increase of the relative static dielectric permittivity of the δ-layer due to the changing of its composition increasing oxidation time (see expressions (8) and (11)).

Conclusions

The high-planar epitaxial layers of n-$Pb_{0.935}Sn_{0.065}Te_{0.243}Se_{0.757}$ quaternary solid solutions, lattice matched with {111}BaF_2 substrates, have been grown from bounded volume of supersaturated melt-solutions in the growth temperature region 773÷873 K by the liquid phase epitaxy technique at a programmatic refrigeration rate of 0.1÷0.2 K/min and a temperature reduction range of ΔT=5÷10 K. The laboratory methodology of the production of Cu/δ-layer/n-$Pb_{0.935}Sn_{0.065}Te_{0.243}Se_{0.757}$/In Schottky barrier structures by thermal vacuum deposition has been developed. The analysis of the dependence of the CVC and FVC on the δ-layer width has shown that: 1) the values of zero bias resistance area product, ideality coefficient, intercept voltage, zero bias built-in potential increase and saturation current, zero bias capacitance decrease with the increasing of δ-layer width; 2) the barrier height depends on the applied voltage bias; 3) the current value at the one and the same voltage bias decreases with the increasing of δ-layer width; 4) the reverse branches of the CVC does not saturate.

References

1. F.F. Sizov, Lead-tin chalcogenide solid solutions and photodetectors on them basis (in Russian) // *Zarubezhnaya Electronnaya Tehnika*, (24), pp. 3-48 (1977).
2. N.N. Berchenko, K.I. Gejman, A.V. Matveenko, p-n junctions and Schottky barriers production methods in the lead chalcogenides and solid solutions on them basis (in Russian) // *Zarubezhnaya Electronnaya Tehnika,* (14), pp.3-70 (1977).
3. N.N. Berchenko, D. Sh. Zaridze, A.V. Matveenko, Formation of the Schottky barriers and heterostructures in the lead chalcogenides and solid solutions on them basis (in Russian) // *Zarubezhnaya Electronnaya Tehnika*, **(4)**, pp. 34-52 (1979).
4. C. Corsi, A. D'amico, G. Petrocco, E. Fainelli, G. Cappuccio, G. Vitali, Electro-optical performance of multylayer epitaxial structures of metal-$Pb_xSn_{1-x}Te$ Schottky diodes // *Thin Solid Films*, **36** (1), pp. 239-242 (1976).
5. S. Buchner, T.S. Sun, W.A. Beck, J.M. Chen, Schottky barrier formation on (Pb, Sn) Te // *J. Vac. Sci. Technol.*, **16** (5), pp. 1171-1173 (1979).
6. B.K. Hohnke, H. Holloway, K.F. Yeung, M.D. Hurley, Thin-film (Pb, Sn) Se photodiodes for 8-12-μm operation // *Appl. Phys. Lett.*, **29** (2), pp. 98-100 (1976).
7. D.A. Gorski, Protective coating for IV-VI compound semiconductor devices // U. S. Patent, July 13, № 3969743 (1976).
8. R.B. Schoolar, J.D. Jensen, Narrow-band detection at long wavelengths with epitaxial $Pb_ySn_{1-y}Se$ films // *Appl. Phys. Lett.*, **31** (8), pp. 536-538 (1977).
9. H. Zogg, C. Maissen, J. Masek, S. Blunier, A. Lambrecht, M. Tacke, Heteroepitaxial $Pb_{1-x}Sn_xSe$ on Si infrared sensor array with 12mm cut-off wavelength // *Appl. Phys. Lett.*, **55** (10), pp. 969-971 (1989).
10. H. Holloway, M.D. Hurley, E.B. Schermer, IV-VI Semiconductor lateral-collection photodiodes // *Appl. Phys. Lett.*, **32** (1), pp. 65-67 (1978).
11. T.A. Grishina, N.N. Berchenko , G.I. Goderdzishvili, I.A. Drabkin, A.V. Matveenko, T.D. Mheidze, D.A. Sakseev, E.A. Tretyakova, Surface barrier structures with intermediate layer on the $Pb_{0.77}Sn_{0.23}Te$ (in Russian) // *J. Tech. Phys.*, **57** (12), pp. 2355-2360 (1987).
12. F.F. Sizov, A.A. Sava, V.V. Tetyorkin, S.G. Bunchuk, S.A. Belokon, Interface and properties of the In(Cu)/PbTe rectifying contacts (in Russian) // *Inorganic Materials*, **26** (6), pp. 1193-1198 (1990).
13. O.A. Alexandrova, A.T. Ahmeganov, R.Tz. Bondokov, V.A. Moshnikov, I.V. Saunin, Yu. M. Tairov, V.I. Shtanov, L.V. Yashina, An investigation of In/n-PbTe barrier structures with a thin intermediate insulator layer (in Russian) // *Physics and Technics of semiconductors,* **34** (12), pp. 1420-1425 (2000).
14. N.N. Berchenko, A.I. Evstigneev, V.Yu. Erohov, A.V. Matveenko, Narrow-band-gap semiconductor surface properties and methods of its protection (in Russian) // *Zarubezhnaya Electronnaya Tehnika,* (3), pp. 3-78 (1981).
15. E.H. Rhoderick, Metal-semiconductor contacts, Clarendon Press, Oxford (1978).
16. S.M. Szi, Physics of Semiconductor Devices, Wiley-Interscience Publication, John Wiley and Sons, New York-Chichester-Brisbane-Toronto-Singapore (1981).
17. V.V. Batavin, Yu.A. Konzevoj, Yu.V. Fedorovich, Properties measurement of the semiconductor materials and structures (in Russian), Radio i svyaz, Moscow (1985).
18. V.I. Strikha, E.V. Buzanyova, Physical foundations of the metal-semiconductor contacts reliability in the integrated electronics (in Russian), Radio i svyaz, Moscow (1987).
19. E.V. Buzanyova, Microstructures of the integrated electronics (in Russian), Radio i svyaz, Moscow (1990).
20. G.P. Peka, V.I. Strikha, Surface and contact effects in the semiconductors (in Ukrainian), Lybid, Kyjiv (1992).